

EVOLUTION OF SYNCHROTRON X-RAYS IN SUPERNOVA REMNANTS

RYOKO NAKAMURA^{1,2}, AYA BAMBA^{3,1,4}, TADAYASU DOTANI¹, MANABU ISHIDA¹, RYO YAMAZAKI⁴, KAZUNORI KOHRI⁵

Draft version November 8, 2018

ABSTRACT

A systematic study of the synchrotron X-ray emission from supernova remnants (SNRs) has been conducted. We selected a total of 12 SNRs whose synchrotron X-ray spectral parameters are available in the literature with reasonable accuracy, and studied how their luminosities change as a function of radius. It is found that the synchrotron X-ray luminosity tends to drop especially when the SNRs become larger than ~ 5 pc, despite large scatter. This may be explained by the change of spectral shape caused by the decrease of the synchrotron roll-off energy. A simple evolutionary model of the X-ray luminosity is proposed and is found to reproduce the observed data approximately, with reasonable model parameters. According to the model, the total energy of accelerated electrons is estimated to be 10^{47-48} ergs, which is well below the supernova explosion energy. The maximum energies of accelerated electrons and protons are also discussed.

Subject headings: acceleration of particles — ISM: supernova remnants — X-rays: ISM

1. INTRODUCTION

Young supernova remnants (SNRs) are widely believed to be the main source of Galactic cosmic rays. Koyama et al. (1995) discovered synchrotron X-rays from shells of SN 1006, which was the first observational clue of cosmic-ray electrons being accelerated up to the TeV energy range. Later, several young SNRs were found to have synchrotron X-ray shells (c.f., Koyama et al. 1997; Slane et al. 1999; Bamba et al. 2000; Vink & Laming 2003). Another piece of evidence for cosmic-ray acceleration in SNRs was obtained from gamma-ray observations. Very-high-energy (VHE) and GeV gamma-rays have been detected from several SNRs, although, it is still unclear whether their origin is hadronic or leptonic (e.g., Aharonian et al. 2004, 2007; Abdo et al. 2010b,c, 2011).

Despite these various pieces of evidence in favor of acceleration, it is still unclear how the acceleration process evolves in SNRs, in particular how the accelerated particles cool down and how they escape from SNRs. One reason for this lack of understanding is that past observational studies have concentrated on individual sources alone. In this paper, we investigate, for the first time, the time evolution of SNR synchrotron X-rays, using all available data in literature for sources in which this emission component is bright. In section 2, we describe the evolution of synchrotron X-ray luminosity in our sample. An interpretation and a simple model to support it are in section 3. Finally, section 4 is devoted to discussion of the results.

2. SAMPLE SELECTION AND RESULTS

We searched the literature for reports of synchrotron X-ray emission from SNRs and found a total of 14 such

sources. However, we could not use all of these for the current study, for various reasons. Kepler (Bamba et al. 2005; Reynolds et al. 2007) and G330.2+1.0 (Park et al. 2009) had to be removed from our sample, because of the difficulty of estimating the total synchrotron X-ray luminosity, caused by a low detection significance or by contamination from thermal X-rays. Thus our sample consists of the 12 SNRs listed in Table 1. We used the latest value of the 2–10 keV synchrotron X-ray unabsorbed flux from the references listed in the table. When the reported flux was not absorption-corrected or was for a different energy band, we normalized it unabsorbed flux in the 2–10 keV using the best-fit model in the references. Synchrotron X-ray emission may have a spectral roll-off in the 2–10 keV band. When significant roll-off was reported in the references, we took such a component into account while computing the flux. Some SNRs (Cas A, Tycho, SN 1006) have bright thermal X-ray emission, which makes it difficult to estimate the synchrotron X-ray flux. In these cases, we inferred the synchrotron X-ray flux based on wide-band information and/or detailed spectroscopy to isolate synchrotron X-rays from thermal component, as we believe such analysis can provide the most reliable results currently available. Two of the sample sources, W28 and G156.7+5.7, are largely extended but were only partly observed with enough exposure in X-rays. As the X-ray luminosities can be deduced only for the observed regions (5% for W28 and 26% for G156.7+5.7, respectively), possible contributions from the unobserved regions are included in the upper error bars. When we estimated these contributions, we assumed that the surface brightness of the unobserved region in each source is identical to that of the observed one. The distance uncertainty is also included into the errors on the luminosity. We used a 10% distance uncertainty for cases where no uncertainty was available in the literature. In summary, we took into account the following uncertainties; statistical errors given in literatures, systematic distance uncertainty, and the limited coverage of the SNR extension.

In order to study the time evolution, we need to know the SNR ages. However, we have only four SNRs whose ages are historically known. Another parameter, the ionization time scale of heated plasma, is also difficult to determine since several SNRs show no thermal emission. We thus use the

¹ ISAS/JAXA Department of High Energy Astrophysics 3-1-1 Yoshinodai, Chuo-ku, Sagami-hara, Kanagawa 252-5210, Japan

² Department of Physics, Tokyo Institute of Technology, 2-12-1 Ookayama, Meguro-ku, Tokyo 152-8551, Japan

³ School of Cosmic Physics, Dublin Institute for Advanced Studies 31 Fitzwilliam Place, Dublin 2, Ireland

⁴ Department of Physics and Mathematics, Aoyama-Gakuin University 5-10-1 Fuchinobe, Sagami-hara, Kanagawa, 252-5258, Japan

⁵ Theory Center, Institute of Particle and Nuclear Studies, KEK (High Energy Accelerator Research Organization), 1-1 Oho, Tsukuba 305-0801, Japan

physical radius of each SNR, R_s , as the age indicator. R_s is taken from Green (2009). The distance uncertainty is included in the error computation. Some SNRs have distorted shapes, as shown in Tab. 1. This is also included in the errors on the radii. All the derived parameters are shown in Tab. 1. The radius of a SNR depends on the density of the interstellar medium, but rather insensitively. For remnants in the Sedov phase, $R_s \propto n_0^{-1/5}$ (where n_0 is the upstream number density). The radius changes by only a factor of ~ 2 even if the upstream density changes by 2 orders of magnitude. The radius also has very weak dependency on the explosion energy E_0 , $R_s \propto E_0^{1/5}$. On the other hand, $R_s \propto t_{\text{age}}^{2/5}$ (where t_{age} is the age of the remnant). Thus the radius is a good age indicator.

Figure 1 shows the synchrotron X-ray luminosity as a function of the radius. One can see that the luminosity is in the order of 10^{34} – 10^{36} ergs s^{-1} when the SNRs are smaller than $R_s \sim 5$ pc, which corresponds to an age of a few hundred years, whereas it decreases to 10^{32} – 10^{35} ergs s^{-1} beyond $R_s \sim 5$ pc. It appears that the luminosity drops off rapidly at $R_s \sim 5$ pc, although the scatter is rather large. Note that all the SNRs with $R_s < 5$ pc display synchrotron X-rays brighter than 10^{34} ergs s^{-1} (Green 2009), whereas most of larger SNRs do not have significant synchrotron X-rays. This fact makes the difference of luminosities larger between the two regions. The drop off in non-thermal X-ray luminosity reaches two or three orders of magnitude, which is much larger than the errors on the individual luminosities. We have carried out a similar analysis for the thermal X-ray luminosity for SNRs in the Large Magellanic Cloud (Williams et al. 1999) and the radio luminosity of Galactic SNRs (Green 2009; Case & Bhattacharya 1998). However, no drop off like that observed for synchrotron X-rays has been found.

3. EVOLUTION OF SYNCHROTRON X-RAYS

Here we consider the cause of the decrease in synchrotron X-ray emission identified in the previous section. The νF_ν -spectrum of synchrotron X-ray radiation has a peak around the roll-off frequency, ν_{roll} , above which the flux rapidly decays towards higher frequencies. As SNRs evolve, ν_{roll} is known to decrease (e.g., Bamba et al. 2005). The observed rapid decay in synchrotron X-rays around $R_s \sim 10$ pc could be caused by ν_{roll} passing through the X-ray band to lower energies. In this section, we discuss this possibility in detail. We introduce essential argument first, and show a simple model to support it later.

We assume that the electron acceleration is energy-loss-limited, in which the maximum energy of electrons, E_e^{max} , is determined from the balance of the synchrotron loss and acceleration:

$$E_e^{\text{max}} = \frac{24}{\xi^{1/2}} \left(\frac{v_s}{10^8 \text{ cm s}^{-1}} \right) \left(\frac{B_d}{10 \mu\text{G}} \right)^{-1/2} \text{ (TeV)}, \quad (1)$$

where ξ is the gyro-factor. In deriving Eq. (1), we equate the acceleration time, $t_{\text{acc}}(E) = 20\xi cE/3ev_s^2 B_d$ with the synchrotron cooling time, $t_{\text{syn}}(E) = 125 \text{ yr}(E/10 \text{ TeV})^{-1}(B_d/100 \mu\text{G})^{-2}$, where v_s and B_d are the shock velocity and the downstream magnetic field, respectively. In this case, we derive

$$h\nu_{\text{roll}} \sim 0.4 \text{ keV } \xi^{-1} (v_s/10^8 \text{ cm s}^{-1})^2, \quad (2)$$

which is independent of B_d (e.g., Aharonian & Atoyan 1999; Yamazaki et al. 2006). The roll-off frequency and the shock

velocity have been measured in several SNRs (Cas A, SN 1006; Reynolds & Keohane 1999; Patnaude & Fesen 2009; Bamba et al. 2008; Ghavamian et al. 2002). For these SNRs, eq.(2) is consistent with the observational values to within 1 order of magnitude assuming $\xi = 1$. Also note that the effect of particle escape from the shock region (e.g., Reynolds 1998; Ohira et al. 2010) is not considered in this paper. This effect might be important for older SNRs (Ohira et al. 2011). However, our present model reproduces the observed trend well, suggesting that particle escape is not yet significant for these SNRs (see also the last paragraph in section 4).

The X-ray spectrum of synchrotron radiation is well approximated analytically. It is mainly determined by shock dynamics in the SNR if the synchrotron X-ray-emitting electrons with energy E satisfy $t_{\text{syn}}(E) < t_{\text{age}}$, where t_{age} is the age of the SNR. In this case, the energy spectrum of electrons is generally given by

$$N_e(E) = AE^{-p}(1 + E/E_b)^{-1} \exp[-(E/E_e^{\text{max}})^2], \quad (3)$$

where the break energy, E_b , is determined by $t_{\text{syn}}(E_b) = t_{\text{age}}$. During the acceleration, electrons with $E > E_b$ suffer energy loss via synchrotron cooling, which causes a steepening of the energy spectrum (e.g., Longair 1994). We also note that the shape of the cutoff is analytically obtained in Zirakashvili & Aharonian (2007). Given the electron distribution, we calculate the approximate formula of the X-ray luminosity, L_ν . The characteristic frequency, $\nu_{\text{syn}}(E)$, of the synchrotron radiation emitted by electrons with energy E is given by

$$h\nu_{\text{syn}}(E) \sim 0.12 \text{ keV}(B_d/10 \mu\text{G})(E/10 \text{ TeV})^2. \quad (4)$$

Then, as long as $\nu < \nu_b = \nu_{\text{syn}}(E_b)$, we can apply the standard formula, $L_\nu \propto AB_d^{(p+1)/2} \nu^{-(p-1)/2}$ (e.g., Longair 1994). On the other hand, if $\nu_b < \nu$, the spectral slope steepens ($L_\nu \propto \nu^{-p/2}$) due to the steepening of the electron distribution, and we derive

$$\begin{aligned} L_\nu &\propto AB_d^{(p+1)/2} \nu_b^{-(p-1)/2} (\nu/\nu_b)^{-p/2} \exp(-\sqrt{\nu/\nu_{\text{roll}}}) \\ &\propto AB_d^{(p-2)/2} \nu^{-p/2} \exp(-\sqrt{\nu/\nu_{\text{roll}}}), \end{aligned} \quad (5)$$

where we assume that L_ν is continuous at $\nu = \nu_b$, and we again use the result of Zirakashvili & Aharonian (2007) for the cutoff shape. Calculating ν_b as

$$h\nu_b \sim 0.19 \text{ keV}(B_d/10 \mu\text{G})^{-3}(t_{\text{age}}/10^4 \text{ yr})^{-2}, \quad (6)$$

we find that throughout the evolution of the SNR, the X-ray band (2–10 keV) always lies above ν_b because for young SNRs ($t_{\text{age}} \lesssim 10^3$ yr), the magnetic field may be amplified to $B_d \gg 10 \mu\text{G}$ (e.g., Bamba et al. 2003, 2005; Vink & Laming 2003). Equation. (5) is thus a good approximation of the X-ray luminosity for any arbitrary epoch. In particular, when $p \approx 2$, the X-ray luminosity is insensitive to the magnetic field, depending instead mainly on ν_{roll} . As the SNR ages, the shock velocity v_s decreases and ν_{roll} becomes smaller. Equation (2) tells us that ν_{roll} is below the X-ray band (2–10 keV) when $v_s \lesssim 10^8 \text{ cm s}^{-1}$, so that the X-ray luminosity drops off.

In order to demonstrate the above argument, we construct a simple model to calculate the synchrotron X-ray flux. In our model, a simple shock dynamics scenario is considered. We assume that the forward shock velocity of SNRs v_s is a

function of the age of SNR t_{age} as follows:

$$v_s = \begin{cases} v_i & (t_{age} < t_1; \text{Free expansion phase}), \\ v_i \left(\frac{t_{age}}{t_1}\right)^{-3/5} & (t_1 < t_{age} < t_2; \text{Sedov phase}), \\ v_i \left(\frac{t_2}{t_1}\right)^{-3/5} \left(\frac{t_{age}}{t_2}\right)^{-2/3} & (t_2 < t_{age}; \text{Radiative phase}), \end{cases} \quad (7)$$

$$t_1 = 2.1 \times 10^2 (E_{51}/n_0)^{1/3} v_{i,9}^{-5/3} \text{ yr}, \quad (8)$$

$$t_2 = 4 \times 10^4 E_{51}^{4/17} n_0^{-9/17} \text{ yr}, \quad (9)$$

where $v_i = v_{i,9} \times 10^9 \text{ cm s}^{-1}$, $E_{ej} = E_{51} \times 10^{51} \text{ erg}$, and n_0 are the initial velocity, initial energy of ejecta, and the upstream number density, respectively (e.g., Blondin et al. 1998; Yamazaki et al. 2006). The model assumes that the SNR forward shock propagates into a homogeneous medium. This is, however, not always in the case, since the SNRs could be located inside of superbubbles made by pre-explosion stellar winds. More detailed models for core-collapsed type SNRs, such as RCW 86 (e.g., Vink et al. 1997), should be applied. But it is left for future work.

As illustrated above, the X-ray luminosity has little dependence on the magnetic field. Nevertheless, we model the evolution of the downstream magnetic field, B_d , as follows. Usually, the amplified magnetic field B_{amp} is simply assumed to scale with v_s (Völk et al. 2005; Vink 2008), because magnetic field evolution remains ill-understood. Here we adopt an assumption similar to Völk et al. (2005), leading to a dependence of $B_d \propto v_s$. Let the energy density of the amplified magnetic field $U_B = B_{amp}^2/8\pi$ be proportional to the thermal energy density U_{th} ,

$$\frac{B_{amp}^2}{8\pi} = \epsilon_B U_{th} = \frac{3}{2} \epsilon_B r n_0 k T_d, \quad ,$$

where ϵ_B , r , and kT_d are the energy-partition parameter, a compression ratio, and a downstream temperature obtained by the Rankine-Hugoniot equation $kT_d = [(r-1)/r^2] m_p v_s^2$, respectively. Then, we obtain $B_{amp} = [12\pi m_p (r-1) \epsilon_B n_0 / r]^{1/2} v_s$. The downstream magnetic field is thus given by $B_d = \max\{B_{amp}, r B_{ISM}\}$, where $B_{ISM} = 10 \mu\text{G}$ is the field strength in the interstellar matter.

For given t_{age} , we calculate v_s according to Eq. (7), the shock radius R_s by the integration of v_s , and the luminosity of synchrotron X-rays numerically by using the value of B_d and the electron distribution given by Eqs. (1) and (3). We adopt $E_{51} = v_{i,9} = 1$, $p = 2.0$, $r = 4$, $\xi = 1$, and $\epsilon_B = 0.01$ as fiducial parameters. Note that for $\epsilon_B \sim 0.01$, the evolution of the amplified magnetic field in young SNRs is approximately reproduced (Völk et al. 2005). This is also consistent with previous observational implications for SNRs (Ghavamian et al. 2002; Bamba et al. 2003; Parizot et al. 2006). One finds that with the above assumption for the magnetic field, the cooling time of synchrotron X-ray-emitting electrons is always smaller than the SNR age, t_{age} , so that the X-ray luminosity is well approximated by Eq. (5). Also note that the value of ξ is near unity, implying that acceleration is near the Bohm limit. We assume that the normalization factor of the electron distribution A is constant with time. This is justified if the amount of accelerated particles is proportional to the product of the fluid ram pressure and the SNR volume, that is, $A \propto (n_0 v_s^2) R_s^3$. In the Sedov phase ($R_s \propto t^{2/5}$) during which v_{roll} crosses the X-ray band, we find that A is constant with time.

Fig. 1 shows the results for $n_0 = 5.0, 1.0$, and 0.1 cm^{-3} . For the first two cases, we set $A = 9.0 \times 10^{45} (n_0/1 \text{ cm}^{-3})$, whereas $A = 9.0 \times 10^{45}$ for $n_0 = 0.1 \text{ cm}^{-3}$. A is expressed in the cgs units. One can see that our model roughly reproduces the observed trend with reasonable model parameters. The assumed density, $n_0 = 0.1 - 5.0 \text{ cm}^{-3}$, is typical for the interstellar medium around SNRs, although there are discrepancies for some individual samples. Some SNRs are likely to be located in bubbles or very low density regions. For example, Vink et al. (1997) showed that RCW 86 is in a super-bubble and expands into extremely low density materials. As a result, this SNR should have a very large radius compared with its age. A is also a free parameter which may change from source to source. Adjusting A to within 1 order of magnitude, it is possible to find a solution for the observed density in each case. Since our aim is simply to reproduce the overall evolutionary trend in an approximate manner, we ignore such fluctuations in this work.

4. DISCUSSION

We have reproduced the observed fast drop-off in synchrotron X-ray luminosity with SNR radius using a quite simple model. Recently, Patnaude et al. (2011) discovered a decline of a few percent in the synchrotron X-ray power from one source, Cas A, and reached a similar conclusion.

The total and maximum energy of accelerated particles can be derived from our model. With the adopted values of A and Eq. (3), we can calculate the total energy of accelerated electrons with the energy above $m_e c^2$ to be $10^{47} - 10^{48}$ ergs, which is reasonable since this range is much smaller than E_{ej} . Note that these estimated values could increase by 1 order of magnitude if we increase ξ by up to 10. Even if we alter the value of p , the results remain similar if we appropriately reset the normalization A . This is expected from equation (5). For example, the results for $p = 2.2$ are almost perfectly in agreement with the case of $p = 2.0$ if we choose $A = 1.7 \times 10^{46} (n_0/1 \text{ cm}^{-3})$ $n_0 = 5.0$ and 1.0 cm^{-3} and $A = 1.7 \times 10^{46}$ for $n_0 = 0.1 \text{ cm}^{-3}$. In these cases, the total energy of accelerated electrons with energy above $m_e c^2$ is again $10^{47} - 10^{48}$ ergs. Bamba et al. (2003) estimated the energy of injected accelerated electrons in SN 1006 for the first time. This was found to be $\sim 10^{44} - 10^{45}$ ergs per small segments of filaments, although with rather large uncertainty. The total energy of accelerated electrons is approximately $10^{46} - 10^{48}$ ergs considering the size of these segments, which is consistent with our result. Bamba et al. (2005) show that the energy injected into accelerated electrons is always similar in young SNRs, which is also consistent with our results. Theoretically, Berezhko & Völk (2006) estimated the energy injected into accelerated protons to be 10^{50} ergs in the case of RX J1713-3946. This is also consistent with our results when we consider the electron and proton ratio of 10^{-4} in cosmic rays.

At present, no direct information on the accelerated protons is obtained by X-ray observations. One might consider whether we could estimate the total energy of accelerated protons under the assumption of a similar A as for electrons. However, this is not possible because the injection efficiency is different in each case. On the other hand, the maximum energy of accelerated protons, E_p^{max} , can be estimated according to our model. The synchrotron and π^0 -decay loss timescales are negligible for protons, and thus E_p^{max} is determined by the

condition $t_{\text{acc}} = t_{\text{age}}$, and we obtain

$$E_p^{\text{max}}(t_{\text{age}}) = \frac{4.8 \times 10^2}{\xi} \left(\frac{v_s}{10^9 \text{ cm s}^{-1}} \right)^2 \left(\frac{B_d}{10 \mu\text{G}} \right) \left(\frac{t_{\text{age}}}{10^3 \text{ yr}} \right) \text{ TeV}. \quad (10)$$

Although the effect of the wave damping and/or escape may be significant in older systems (e.g., Zirakashvili & Aharonian 2007; Ohira et al. 2010), we ignore it here for simplicity. Figure 2 shows E_p^{max} as a function of t_{age} . In the free expansion phase, E_p^{max} increases in proportion to the age, and protons are accelerated quickly up to around the knee energy in ~ 100 yr. When the shock velocity decreases, E_p^{max} becomes smaller. Hence E_p^{max} peaks at $t_{\text{age}} = t_1$. In contrast to the case of electron acceleration, $E_p^{\text{max}}(t_1)$ (that is the maximum of E_p^{max}) is larger for higher upstream density n_0 , and it changes only within a factor of ~ 2 for $n_0 = 0.1\text{--}5.0 \text{ cm}^{-3}$. Since $B_d \propto n_0^{1/2}$ and $t_1 \propto n_0^{-1/3}$, one finds $E_p^{\text{max}}(t_1) \propto B_d t_1 \propto n_0^{1/6}$. Protons are accelerated up to $E_p^{\text{max}}(t_1) \sim 10^{15\text{--}16}$ eV in any SNR, with little density dependence. This result might be important for explaining the break at $\sim 10^{15.5}$ eV in the observed cosmic-ray spectrum with the shock acceleration on SNRs. On the other hand, one can find $E_e^{\text{max}} \propto B_d^{-1/2} v_s \propto v_s^{1/2}$ if $B_d = B_{\text{amp}} \propto v_s$. Hence the maximum energy of electrons scales as $E_e^{\text{max}} \propto t^0$ and $\propto t^{-3/10}$ for the free expansion and Sedov phases, respectively, so that it depends only weakly on the SNR age.

Recent *Fermi* observations of middle-aged SNRs have

shown the presence of a gamma-ray spectral break around energies of a few GeV (e.g., Abdo et al. 2009, 2010a). Several interpretations have been given (e.g., Inoue et al. 2010; Li & Chen 2010, 2011; Ohira, Murase, Yamazaki 2011), one of which is the escape of particles from acceleration sites. In this scenario, accelerated particles with energies of more than about 10-100 GeV have already escaped from the acceleration region (Ohira, Murase, Yamazaki 2011). In contrast, our present model has shown that even for $t_{\text{age}} \gtrsim 10^4$ yr, ~ 10 TeV electrons still exist around the shock front (see Figure 2). This apparent discrepancy may come from the fact that most SNRs observed by *Fermi* are interacting with molecular clouds, whereas in our sample there is only one (W 28) undergoing such a collision. Hence molecular clouds may play an important role in dispersing cosmic rays from the SNR shock into the interstellar matter.

We would like to thank the anonymous referee for the fruitful comments. We also thank S. Wagner and G. Pühlhofer for the analysis of individual sources. We also thank P. Gandhi for the English correction. This work was supported in part by Grant-in-Aid for Scientific Research of the Japanese Ministry of Education, Culture, Sports, Science and Technology (MEXT) of Japan, No. 22684012 (A. B.), No. 21740184 and 21540259 (R. Y.) and No. 18071001, 22244030, and 21111006 (K. K.). K.K. was partly supported by the Center for the Promotion of Integrated Sciences (CPIS) of Sokendai.

REFERENCES

- Abdo, A. A. et al. 2009, *ApJ*, 706, L1
 Abdo, A. A. et al. 2010a, *Science*, 327, 1103
 Abdo, A. A., et al. 2010, *ApJ*, 718, 348
 Abdo, A. A., et al. 2010, *ApJ*, 710, L92
 Abdo, A. A., et al. 2011, *ApJ*, 734, 28
 Aharonian, F. A., & Atoyan, A. M. 1999, *A&A*, 351, 330
 Aharonian, F. A., et al. 2004, *Nature*, 432, 75
 Aharonian, F., et al. 2007, *ApJ*, 661, 236
 Bamba, A., Tomida, H., & Koyama, K. 2000, *PASJ*, 52, 1157
 Bamba, A., Ueno, M., Koyama, K., & Yamauchi, S. 2001, *PASJ*, 53, L21
 Bamba, A., Yamazaki, R., Ueno, M., & Koyama, K. 2003, *ApJ*, 589, 827
 Bamba, A., Yamazaki, R., Yoshida, T., Terasawa, T., & Koyama, K. 2005, *ApJ*, 621, 793
 Bamba, A., et al. 2008, *PASJ*, 60, 153
 Berezhko, E. G., & Völk, H. J. 2006, *A&A*, 451, 981
 Blondin, J. M., Wright, E. B., Borkowski, K. J., & Reynolds, S. P. 1998, *ApJ*, 500, 342
 Case, G. L., & Bhattacharya, D. 1998, *ApJ*, 504, 761
 Caswell, J. L., Murray, J. D., Roger, R. S., Cole, D. J., & Cooke, D. J. 1975, *A&A*, 45, 239
 Fukui, Y., et al. 2003, *PASJ*, 55, L61
 Gerardy, C. L., & Fesen, R. A. 2007, *MNRAS*, 376, 929
 Ghavamian, P., Winkler, P. F., Raymond, J. C., & Long, K. S. 2002, *ApJ*, 572, 888
 Green, D. A. 2009, *Bulletin of the Astronomical Society of India*, 37, 45
 Helder, E. A., & Vink, J. 2008, *ApJ*, 686, 1094
 Inoue, T. et al. 2010, *ApJ*, 723, L108
 Katsuda, S., Petre, R., Hwang, U., Yamaguchi, H., Mori, K., & Tsunemi, H. 2009, *PASJ*, 61, 155
 Koyama, K., Petre, R., Gotthelf, E. V., Hwang, U., Matsura, M., Ozaki, M., & Holt S. S. 1995, *Nature*, 378, 255
 Koyama, K., Kinugasa, K., Matsuzaki, K., Nishiuchi, M., Sugizaki, M., Torii, K., Yamauchi, S., & Aschenbach, B. 1997, *PASJ*, 49, L7
 Krause, O., Tanaka, M., Usuda, T., Hattori, T., Goto, M., Birkmann, S., & Nomoto, K. 2008, *Nature*, 456, 617
 Lazendic, J. S., Dewey, D., Schulz, N. S., & Canizares, C. R. 2006, *ApJ*, 651, 250
 Li, H., & Chen, Y. 2010, *MNRAS*, 409, L35
 Li, H., & Chen, Y. 2011, arXiv:1108.4541
 Longair, M. S. 1994, *High Energy Astrophysics, 2, Stars, the Galaxy and the interstellar medium* (Cambridge: Cambridge University Press)
 Nakamura, R., Bamba, A., Ishida, M., Nakajima, H., Yamazaki, R., Terada, Y., Pühlhofer, G., & Wagner, S. J. 2009, *PASJ*, 61, 197
 Ohira, Y., Murase, K., & Yamazaki, R. 2010, *A&A*, 513, A17
 Ohira, Y., Murase, K., & Yamazaki, R. 2011a, *MNRAS*, 410, 1577
 Ohira, Y., Yamazaki, R., Kawanaka, N., & Ioka, K. 2011b, arXiv:1106.1810
 Parizot, E., Marcowith, A., Ballet, J., & Gallant, Y. A. 2006, *A&A*, 453, 387
 Park, S., Kargaltsev, O., Pavlov, G. G., Mori, K., Slane, P. O., Hughes, J. P., Burrows, D. N., & Garmire, G. P. 2009, *ApJ*, 695, 431
 Patnaude, D. J., & Fesen, R. A. 2009, *ApJ*, 697, 535
 Patnaude, D. J., Vink, J., Laming, J. M., & Fesen, R. A. 2011, *ApJ*, 729, L28
 Reed, J. E., Hester, J. J., Fabian, A. C., & Winkler, P. F. 1995, *ApJ*, 440, 706
 Reynolds, S. P. 1998, *ApJ*, 493, 375
 Reynolds, S. P., Borkowski, K. J., Hwang, U., Hughes, J. P., Badenes, C., Laming, J. M., & Blondin, J. M. 2007, *ApJ*, 668, L135
 Reynolds, S. P., Borkowski, K. J., Green, D. A., Hwang, U., Harrus, I., & Petre, R. 2008, *ApJ*, 680, L41
 Reynolds, S. P., & Keohane, J. W. 1999, *ApJ*, 525, 368
 Rosado, M., Ambrocio-Cruz, P., Le Coarer, E., & Marcelin, M. 1996, *A&A*, 315, 243
 Seward, F., Gorenstein, P., & Tucker, W. 1983, *ApJ*, 266, 287
 Slane, P., Gaensler, B. M., Dame, T. M., Hughes, J. P., Plucinsky, P. P., & Green, A. 1999, *ApJ*, 525, 357
 Tamagawa, T., et al. 2009, *PASJ*, 61, 167
 Velázquez, P. F., Dubner, G. M., Goss, W. M., & Green, A. J. 2002, *AJ*, 124, 2145
 Vink, J., Kaastra, J. S., & Bleeker, J. A. M. 1997, *A&A*, 328, 628
 Vink, J., & Laming, J. M. 2003, *ApJ*, 584, 758
 Vink, J., Bleeker, J., van der Heyden, K., Bykov, A., Bamba, A., & Yamazaki, R. 2006, *ApJ*, 648, L33
 Vink, J. 2008, in *AIP Conf. Ser. 1085, Proc. 4th International Meeting on High Energy Gamma-Ray Astronomy*, ed. F. A. Aharonian et al. (Melville, NY: AIP), 169
 Völk, H. J. et al. 2005, *A&A*, 433, 229
 Williams, R. M., Chu, Y.-H., Dickel, J. R., Petre, R., Smith, R. C., & Tawarez, M. 1999, *ApJS*, 123, 467
 Winkler, P. F., Gupta, G., & Long, K. S. 2003, *ApJ*, 585, 324

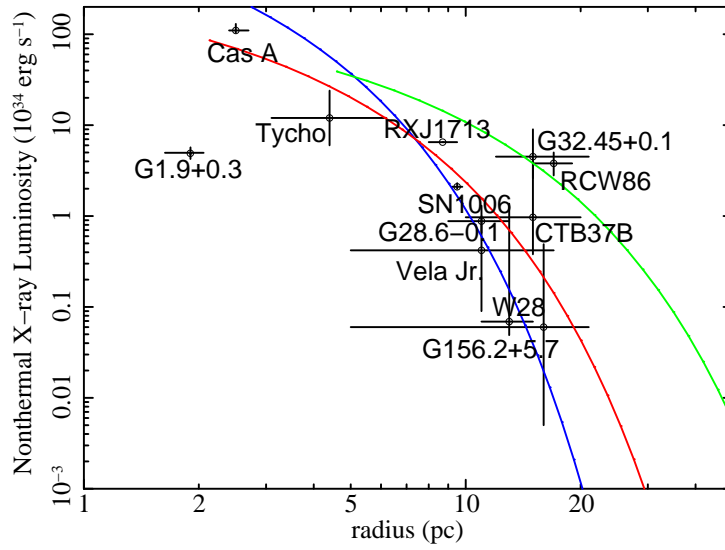


FIG. 1.— Synchrotron X-ray luminosity in 2–10 keV band as a function of radius for Galactic SNRs. Solid lines represent the evolutionary model of synchrotron X-rays for n_0 of 5.0 cm^{-3} (blue), 1.0 cm^{-3} (red), and 0.1 cm^{-3} (green). We plot results only for the Sedov phase ($t_1 < t_{\text{age}} < t_2$), in which the normalization of the electron energy distribution, A , is expected to be constant with time (see text for details).

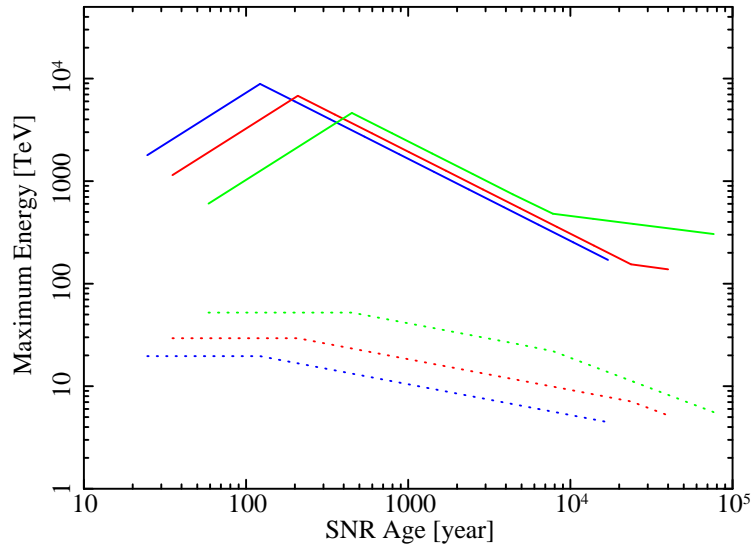


FIG. 2.— The maximum energies of accelerated protons (solid) and electrons (dotted) as functions of the SNR age. The colors match those in Fig. 1.

Yamaguchi, H., Ueno, M., Koyama, K., Bamba, A., & Yamauchi, S. 2004, PASJ, 56, 1059
 Yamaguchi, H., et al. 2008, PASJ, 60, 141
 Yamauchi, S., Koyama, K., Tomida, H., Yokogawa, J., & Tamura, K. 1999, PASJ, 51, 13

Yamazaki, R., Kohri, K., Bamba, A., Yoshida, T., Tsuribe, T., & Takahara, F. 2006, MNRAS, 371, 1975
 Zirakashvili, V. N., & Aharonian, F. 2007, A&A, 465, 695

TABLE 1
OBSERVATIONAL JOURNALS AND PHYSICAL PARAMETERS FOR SNRS WITH SYNCHROTRON
X-RAYS.

Target	Distance (kpc)	Size (arcmin)	Radius (pc)	L_X^a (10^{34} ergs s^{-1})	References
G1.9+0.3	8.5	1.5	1.9	$4.9^{+0.1}_{-0.2}$	(1)
Cas A	$3.4^{+0.3}_{-0.1}$	5	$2.5^{+0.2}_{-0.1}$	110^{+20}_{-6}	(2) (3) (4)
Tycho	$3.8^{+1.5}_{-1.1}$	8	$4.4^{+1.8}_{-1.3}$	12^{+2}_{-6}	(5) (6) (7)
RX J1713–3946	1.0	65×55	$8.7^{+0.8}_{-0.7}$	6.5	(8) (9)
SN 1006	2.2 ± 0.1	30	9.5 ± 0.3	$2.1^{+0.2}_{-0.1}$	(10) (11) (12)
G28.6–0.1	$7.0^{+1.5}_{-1.0}$	13×9	11 ± 2	$0.88^{+0.42}_{-0.23}$	(13)
Vela Jr.	0.65 ± 0.35	120	11 ± 6	$0.42^{+0.58}_{-0.33}$	(14)
W28	1.9 ± 0.3	48	13 ± 2	$0.069^{+1.3}_{-0.02}$ ^b	(15) (16)
CTB 37B	10.2 ± 3.5	10 ^c	15 ± 5	$0.97^{+3.1}_{-0.59}$	(17) (18)
G32.45+0.1	17^{+7}_{-4}	6	15^{+6}_{-5}	$4.5^{+4.5}_{-1.9}$	(19)
G156.2+5.7	$1.0^{+0.3}_{-0.7}$	110	16^{+5}_{-11}	$0.060^{+0.43}_{-0.055}$ ^b	(20) (21) (22)
RCW 86	2.8 ± 0.4	42	17 ± 2	$3.8^{+1.2}_{-1.0}$	(23) (24) (25)

NOTE. — (1) Reynolds et al. (2008); (2) Reed et al. (1995); (3) Helder & Vink (2008); (4) Lazendic et al. (2006); (5) Krause et al. (2008); (6) Tamagawa et al. (2009); (7) Seward et al. (1983); (8) Fukui et al. (2003); (9) Slane et al. (1999); (10) Winkler et al. (2003); (11) Bamba et al. (2008); (12) Yamaguchi et al. (2008); (13) Bamba et al. (2001); (14) Aharonian et al. (2007); (15) Velázquez et al. (2002); (16) Nakamura et al., submitted; (17) Caswell et al. (1975); (18) Nakamura et al. (2009); (19) Yamaguchi et al. (2004); (20) Gerardy & Fesen (2007); (21) Yamauchi et al. (1999); (22) Katsuda et al. (2009); (23) Rosado et al. (1996); (24) Bamba et al. (2000); (25) Vink et al. (2006)

^a In the 2–10 keV band.

^b The upper-bound of X-ray luminosity is calculated with the assumption that the SNR uniformly emits synchrotron X-rays, since present observations do not cover the entire remnant.

^c The size of radio partial shell is used.